In Situ Synthesis of Poly(ethylene terephthalate) (PET) in Ethylene Glycol Containing Terephthalic Acid and Functionalized Multiwalled Carbon Nanotubes (MWNTs) as an Approach to MWNT/PET Nanocomposites

Hwa-Jeong Lee,[†] Se-Jin Oh,[†] Ja-Young Choi,[†] Jin Won Kim,[‡] Jungwan Han,[‡] Loon-Seng Tan,[§] and Jong-Beom Baek*,[†]

School of Chemical Engineering, Chungbuk National University, Cheongju, Chungbuk, 361-763 South Korea, Saehan Industry Inc., Gumi, Kyungbook, 730-707 South Korea, and Polymer Branch, Materials & Manufacturing Directorate, AFRL/MLBP, Air Force Research Laboratory, Wright-Patterson Air Force Base, Dayton, Ohio 45433

Received June 8, 2005. Revised Manuscript Received July 31, 2005

Multiwalled carbon nanotubes (MWNTs) (diameter range, 10−20 nm) were functionalized with 4-methoxybenzoic acid and 4-ethoxybenzoic acid via a Friedel−Crafts reaction in polyphosphoric acid to afford methoxybenzoyl- and ethoxybenzoyl-functionalized MWNTs. As-received MWNT, methoxybenzoyl-functionalized (MeO-MWNT), and ethoxybenzoyl-functionalized (EtO-MWNT) nanotubes were dispersed in ethylene glycol (EG). Because of the structural similarity, the mixture of EtO-MWNT (0.4 wt %) and EG was a homogeneous dispersion, whereas MeO-MWNT and pristine MWNT were dispersed in EG rather heterogeneously at the same loading. *In situ* polycondensation of EG and terephthalic acid in the presence of pristine MWNT, MeO-MWNT, or EtO-MWNT was carried out to generate the corresponding MWNT/PET, MeO-MWNT/PET, and EtO-MWNT/PET nanocomposites. High molecular weight poly(ethylene terephthalates) (PETs), with intrinsic viscosity range 0.6−0.7 dL/g (*o*-chlorophenol at 30 ± 0.1 °C), were obtained in all cases. In comparing the images from scanning electron microscopy (SEM) taken at the same magnification for these nanocomposites, it is clear that the MWNT/PET system has poor MWNT dispersion and the MeO-MWNT/PET system has a better dispersion. However, EtO-MWNT in PET matrix is most homogeneously dispersed, and the interfacial boundary between EtO-MWNT and PET matrix is practically nondiscernible.

Introduction

When carbon nanotubes (CNTs) are used as reinforcing additives, the resultant nanocomposites are expected to possess much improved properties. However, to achieve maximum enhanced physical properties through such nanoscale additives, there are two fundamental issues needed to be addressed first, and they are related to (i) the effective aspect ratio, largely determined by the state of dispersion,[1] and (ii) interfacial adhesion between additives and matrix.[2] Thus, there have been many efforts to provide homogeneous dispersion of CNTs in various matrix materials via physical,[3] chemical,[4] or combined approaches.[5] However, a homogeneous dispersion aided by a physical method, e.g. sonication, tends to impart structural damages to CNTs with respect to the exposure time and power level.[6] Furthermore, another concern is that the desired material properties of a nanocomposite invariably depend on the strength of specific interactions between CNTs and matrix polymers.[1−3] Thus, covalent and/or noncovalent interactions between CNT and matrix in a nanocomposite are necessary to strengthen the reinforcement effect even after homogeneous CNT dispersion could be achieved. Solubilizing CNTs with suitable chemical groups attached to their surfaces can hinder close lateral contacts among the nanotubes, enable higher degrees of exfoliation, and allow isotropically reinforced nanocomposites to be prepared.[7] In this regard, the chemical modification of CNTs is more viable. CNTs, however, are

* Corresponding author. Tel: +82-43-261-2489. Fax: + 82-43-262-2380. E-mail: jbbaek@chungbuk.ac.kr.
[†] Chungbuk National University.
[‡] Saehan Industry Inc.
[§] Wright-Patterson Air Force Base.

(1) Song, Y. S.; Youn, J. R. *Carbon* **2005**, *43*, 1378.
(2) (a) Ajayan, P. M.; Schadler, L. S.; Giannaris, C.; Rubio, A. *Adv. Mater.* **2000**, *12*, 750. (b) Calvert, P. *Nature* **1999**, *399*, 210. (c) Lourie, O.; Wagner, H. D. *J. Mater. Res.* **1998**, *13*, 2418. (d) Cadek, M.; Coleman, J. N.; Ryan, K. P.; Nicolosi, V.; Bister, G.; Fonseca, A.; Nagy, J. B.; Szostak, K.; Béguin, F.; Blau, W. J. *Nano Lett.* **2004**, *4*, 353.
(3) (a) Zhang, W. D.; Shen, L.; Phang, I. Y.; Liu, T. *Macromolecules* **2004**, *37*, 256. (b) Liu. T.; Phang, I. Y.; Shen, L.; Chow, S. Y.; Zhang, W. D. *Macromolecules* **2004**, *37*, 7214. (c) Andrews, R.; Jacques, D.; Rao, A. M.; Rantell, T.; Derbyshire, F.; Chen, Y.; Chen, J.; Haddon, R. C. *Appl. Phys. Lett.* **1999**, *75*, 1329. (d) Qian, D.; Dickey, E. C.; Andrews, R.; Rantell, T. *Appl. Phys. Lett.* **2000**, *76*, 2868. (e) Shaffer, M. S. P.; Windle, A. H. *Adv. Mater.* **1999**, *11*, 937. (f) Zin, L.; Bower, C.; Zhou, O. *Appl. Phys. Lett.* **1998**, *73*, 1197. (g) Haggenmueller, R.; Gommans, H. H.; Rinzler, A. G.; Fischer, J. E.; Winey, K. I. *Chem. Phys. Lett.* **2000**, *330*, 219. (h) Chen, G. Z.; Shaffer, M. S. P.; Coleby, D.; Dixon, G.; Zhou, W.; Fray, D. J.; Windle, A. H. *Adv. Mater.* **2000**, *12*, 522. (i) Dupire, M.; Michel, J. European Patent 1,054,036A1, November 22, 2000. (j) Sandler, J.; Shaffer, M. S. P.; Prasse, T.; Bauhofer, W.; Schulte, K.; Windle, A. H. *Polymer* **1999**, *40*, 5967. (k) Part, C.; Ounaies, Z.; Watson, K. A.; Crooks, R. E.; Smith, J., Jr.; Lowther, S. E.; Connell, J. W.; Siochi, E. J.; Harrison, J. S.; St. Clair, T. L. *Chem. Phys. Lett.* **2002**, *364*, 303.

10.1021/cm051218t CCC: $30.25
Published on Web 09/03/2005

generally inert and chemically resistant. A common approach to covalent modification of CNTs requires harsh reaction conditions in strong acids such as nitric acid and sulfuric acid and/or their mixtures at elevated temperatures. Significant damage to the molecular framework of CNTs, such as sidewall opening, breaking, and turning into amorphous carbon, are inevitable.[8] Thus, developing an efficient chemical modification method without or with little damage to the surface of CNTs is very important for the development of the ultimate CNT nanocomposites.

Recently, we have developed a mild and efficient chemical modification of vapor-grown carbon nanofibers (VGCNFs) via an electrophilic substitution reaction in polyphosphoric acid (PPA)/phosphorus pentoxide (P_2O_5) medium.[9] We found that this method is equally applicable to multiwalled carbon nanotubes (MWNTs). Aside from serving as a Friedel−Crafts catalyst, PPA plays two important roles in the uniform covalent functionalization of CNT/CNF surfaces. Its moderately acidic nature promotes debundling of nanotubes/nanofibers to promote homogeneous dispersion without damaging them, and its viscous character helps to impede CNT/CNF reaggregation after their dispersion.

In this paper, we describe our continuing effort on the functionalization of MWNTs to effect their homogeneous dispersion in ethylene glycol (EG) and one-pot generation of MWNT/poly(ethylene terephthalate) (PET) nanocomposite. Since PET is one of the most important commercial thermoplastics, the effectiveness of our approach in achieving homogeneous dispersion of MWNTs in EG is a critical step toward imparting PET with multifunctionality in the form of MWNT-based nanocomposites. It should be noted that recently Kumar et al. reported their nanocomposite fibers prepared from dry-mixing of vapor-grown carbon nanofibers and PET followed by melt-spinning.[10] The resultant nanocomposites showed good dispersion of VGCNF in the PET matrix; however, significant reduction in the fiber lengths was observed.

Scheme 1. Functionalization of MWNT or VGCNF in Polyphosphoric Acid/P_2O_5[a]

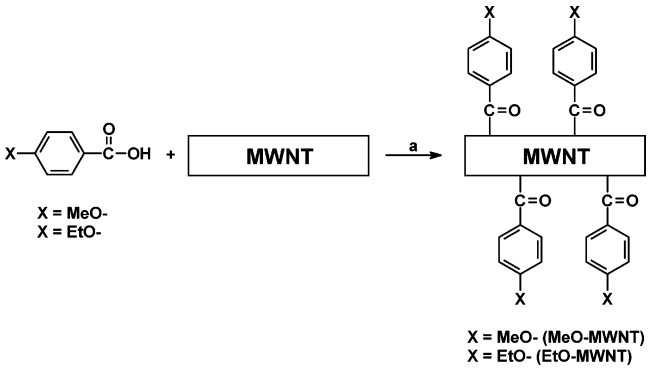

[a] (a) PPA/P_2O_5, 130 °C.

Results and Discussion

Characterization of MWNTs. The average diameter and length of the MWNTs (CVD MWNT 95) were 10−20 nm and 10−50 μm, respectively. The carbon content of the as-received MWNTs was 96.68%, as assayed by elemental analysis. It is noteworthy that the as-received MWNTs, which are prepared by a chemical vapor deposition (CVD) process, contain a little amount of hydrogen (0.15 wt %), presumably attributable to the sp^3C-H and sp^2C-H defects (approximately two such defects per 100 carbon atoms), since hydrocarbon is used as the major component in the feedstock for their productions.[11] On the basis of the rationalization that such C−H bonds would be susceptible to Friedel−Crafts reactions, we have recently reported for the first time that direct and uniform functionalization as well as grafting onto as-received carbon nanomaterials such as MWNTs and VGCNFs are very effective in an optimized PPA/P_2O_5 medium.[9]

Functionalization of MWNT. The reason for 4-methoxybenzoic acid (4-MeO−BA) and 4-ethoxybenzoic acid (4-EtO−BA) being selected was to simply make MWNTs more compatible with PET after functionalization, because the alkoxy and benzoyl units were structurally similar to the PET repeating unit. The structure of ethoxybenzoyl unit is even more so. Thus, the reaction of the respective benzoic acid and MWNTs (1/1, wt/wt ratio) was carried out at approximately 5 wt % of total concentration in PPA/P_2O_5 at 130 °C, as shown in Scheme 1. The initial color of the reaction mixtures was all black, because of the MWNT dispersion. In both cases, the color of the reaction mixtures changed from black to shiny dark brown, as the reaction progressed at elevated temperature. This provided a visual signal that homogeneous dispersion had been achieved and functionalization had indeed occurred. Previously in a model

(4) (a). Sun, Y.-P.; Fu, K.; Lin, Y.; Huang, W. *Acc. Chem. Res.* **2002**, *35*, 1096. (b) Dai, L.; Mau, W. H. *Adv. Mater*. **2001**, *13*, 899. (c) Hirsch, A. *Angew. Chem., Int. Ed.* **2002**, *41*, 1853. (d) Banerjee, S.; Kahn, M. G. C.; Wong, S. S. *Chem. Eur. J.* **2003**, *9*, 1898. (e) Tasis, D.; Tagmatarchis, N.; Georgakilas, V.; Prato, M. *Chem. Eur. J.* **2003**, *9*, 4000. (e) Lin, Y.; Zhou, B.; Shiral Fernando, K. A.; Liu P.; Allard, L. F.; Sun, Y.-P. *Macromolecules* **2003**, *36*, 7199. (f) Mitchell, C. A.; Bahr, J. L.; Arepalli, S.; Tour, J. M.; Krishnamoorti, R. *Macromolecules* **2002**, *35*, 8825.

(5) (a) Huang, W.; Lin, Y.; Taylor, S.; Gaillard, J.; Rao, A. M.; Sun, Y.-P. *Nano Lett.* **2002**, *2*, 231. (b) Sandler, J.; Shaffer, M. S. P.; Prasse, T.; Bauhofer, W.; Schulte, K.; Windle, A. H. *Polymer* **1999**, *40*, 5967. (c) Kumar, S.; Dang, T. D.; Arnold, F. E.; Bhattacharyya, A. R.; Min, B. G.; Zhang, X.; Vaia, R. V.; Park, C.; Wade, W. W.; Hauge, R. H.; Smalley, R. E.; Ramesh, S.; Willis, P. A. *Macromolecules* **2002**, *35*, 9039.

(6) Heller, D. A.; Barone, P. W.; Strano, M. S. *Carbon* **2005**, *43*, 651.

(7) (a) Shaffer, M. S. P.; Fan, X.; Windle, A. H. *Carbon* **1998**, *36*, 1603. (b) Cai, L.; Bahr, J. L.; Yao, Y.; Tour, J. M. *Chem. Mater*. **2002**, *14*, 4235. (c) Mickelson, E. T.; Huffman, C. B.; Rinzler, A. G.; Smalley, R. E.; Hauge, R. H.; Margrave, J. L. *Chem. Phys. Lett*. **1998**, *296*, 188. (d) Bahr, J. L.; Yang, J.; Kosynkin, D. V.; Bronikowski, M. J.; Smalley, R. E.; Tour, J. M. *J. Am. Chem. Soc*. **2001**, *123*, 6536. (e) Bahr, J. L.; Tour, J. M. *Chem. Mater*. **2001**, 13, 3823. (f) Mitchell, C. A.; Bahr, J. L.; Arepalli, S.; Tour, J. M.; Krishnamoorti, R. *Macromolecules* **2002**, *35*, 8825.

(8) (a) Monthioux, M.; Smith, B. W.; Burteaux, B.; Claye, A.; Fischer, J. E.; Luzzi, D. E. *Carbon* **2001**, *39*, 1251. (b) Ko, F.-H.; Lee, C.-Y.; Ko, C.-J.; Chu, T.-C. *Carbon* **2005**, *43*, 727.

(9) (a) Baek, J.-B.; Lyons, C. B.; Tan, L.-S. *J. Mater. Chem*. **2004**, *14*, 2052. (b) Baek, J.-B.; Lyons, C. B.; Tan, L.-S. *Macromolecules* **2004**, *37*, 8278. (c) Oh, S.-J.; Lee, H.-J.; Keum, D.-K.; Lee, S.-W.; Wang, D. H.; Park, S.-Y.; Tan, L.-S.; Baek, J.-B. *Carbon* Submitted (CARBON-D-05-00243).

(10) Ma, H.; Zeng, J.; Realff, M. L.; Kumar, S.; Schiraldi, D. A. *Compos. Sci. Technol*. **2003**, *63*, 1617−1628.

(11) Carneiro, O. S.; Covas. J. A.; Bernardo, C. A.; Calderia, G.; Hattum, F. W. J. V.; Ting, J. M.; Alig, R. L.; Lake, M. L. *Compos. Sci. Technol*. **1998**, *58*, 401.

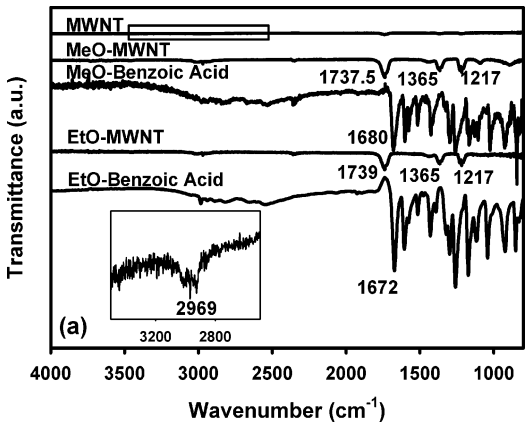

Figure 1. FT-IR (KBr pellet) spectra of samples.

reaction study, the reaction progress of the Friedel−Crafts functionalization process between 2,4,6-trimethylphenoxybenzoic acid and VGCNFs was conveniently monitored by FT-IR,[9a] and we observed that under the reaction conditions, Friedel−Crafts acylation was relatively slow but progressing steadily, as evidenced by the temporal growth of the aromatic ketone ν(C═O) band at 1664 cm^{-1}. The Friedel−Crafts reaction between the methoxybenzoic acid or ethoxybenzoic acid and MWNTs behaved similarly. Both samples were worked up the same way and prior to analysis as follows. The reaction mixture was poured into distilled water. The resulting powdery products were collected by suction filtration, washed with diluted ammonium hydroxide, Soxhlet-extracted with water for 3 days to remove residual PPA and with methanol for three more days to remove unreacted benzoic acids, and finally dried under reduced pressure (0.05 mmHg) for 48 h. Overall yields for MeO-MWNT and EtO-MWNT were 89.8 (at least 39.8 wt % of 4-methoxybenzoyl units attached to MWNT) and 81.0% (at least 31.0 wt % of 4-ethoxybenzoyl units attached to MWNT), respectively. The samples after complete workup were analyzed by FT-IR and identified necessary groups as shown in Figure 1. The FT-IR spectrum of as-received MWNTs has indeed shown small sp^2C-H and sp^3C-H vibrations around 2969 cm^{-1} (Figure 1 inset) that are attributable to the defects at sidewalls and open ends of MWNTs. The defects would provide the preferred sites for an electrophilic substitution reaction. MeO-MWNT sample showed aromatic ketone ν(C═O) at 1738 cm^{-1} (Figure 1), and EtO-MWNT have aromatic ketone ν(C═O) at 1739 cm^{-1} (Figure 1). For comparison purposes, the FT-IR spectra of the starting 4-methoxybenzoic acid and 4-ethoxybenzoic acid are provided (Figure 1). It is clear that the ν(C═O) stretches (1672 and 1680 cm^{-1}) for the starting carboxylic acids are absent in the EtO- and MeO-MWNT spectra.

The SEM images of the pristine MWNT (Figure 2a) show that the tube surfaces are clean and smooth, with average diameter ∼10−20 nm. However, under the same magnification, the surfaces and diameters of functionalized MeO-MWNT and EtO-MWNT (Figure 2, parts b and c, respectively) are distinctly different from the unmodified MWNT (Figure 2a). Both functionalized samples' tube surfaces appear to be heavily and uniformly coated with methoxybenzoyl moiety or ethoxybenzoyl moiety, thus clearly indicative of alkoxybenzoyl units attached to MWNT. Particularly interesting is the observation that the ends of the tubes were heavily sealed with organics and spherically shaped (see Figure 2, indicated with white arrows). This may be due to a larger population of sp^2C-H and greater bond strain at the ends of tubes, which should be more susceptible to the Friedel−Crafts acylation in PPA/P_2O_5 medium. The average diameters of MeO-MWNT and EtO-MWNT have been increased to ∼40 and 45 nm, respectively. The average of these values (∼42 nm) is approximately equivalent to four functionalized MWNT stacked together, assuming that the MWNT diameter is ∼18 nm, as well as that the organics are aligned vertically on the surfaces of MWNT and their lengths are roughly 1 nm.

The observed uniform coating of the MWNT surface by the alkoxybenzoyl groups in the SEM images was very surprising. At this point, we are unable to explain this finding, other than the speculation that there must be other types of reactions occurring in addition to the Friedel−Crafts reaction taking placed at the sp^2C-H defect sites, which alone could not be sufficient for such uniform coverage of the nanotube surfaces with organics.

The TGA study of as-received MWNTs showed that its onset temperature for the weight loss in air and in nitrogen occurred at 600 and 720 °C, respectively (Figure 3a). The thermo-oxidative and thermal degradation of MeO-MWNT and EtO-MWNT under air or nitrogen atmosphere should commence at much lower temperature, because of their organic pendants. The onset temperatures of weight loss for both modified samples started around 420 °C, which was attributed to the loss of arylcarbonyl substituents. The remaining residues at 630 °C were 59 (41% weight loss) and 70% (30% weight loss), for EtO-MWNT and MeO-MWNT, respectively. On the basis of these TGA data, it can be deduced that there are about 3.8 (MeO) or 5.6 (EtO) arylcarbonyl groups covalently attached for every 100 carbon sites on MWNT. However, the elemental analysis results indicated that both MeO-MWNT and EtO-MWNT had about the same degree of functionalization (∼3.5 functionalization per 100 carbon atoms; see Experimental Section). Taking into account that the carbons located in the inner walls (5−20) of MWNT are not accessible to chemical modification, we estimated that the organic pendants on the outermost surface of MWNT are approximately bonded at every two or three carbon sites in order to explain the uniform coating of the nanotube surfaces observed by SEM. This estimation is in contrast to a functionalization in every 20 carbons, as was reported for single walled carbon nanotubes (SWNT).[12] Also, we note that this interpretation goes against the expectation that SWNT should be more reactive than MWNT, since the diameter of SWNT is at least 1 order of magnitude less than MWNT, and therefore should have more curvature strain, which drives the fullerene and CNT reaction chemistry. Further investigation is required to reconcile the analytical data and SEM observation.

Nanocomposite Synthesized from Ethylene Glycol Containing TPA and MWNTs. As depicted in Scheme 2,

(12) Bahr, J. L.; Tour, J. M. *Chem. Mater.* **2001**, *13*, 3823.

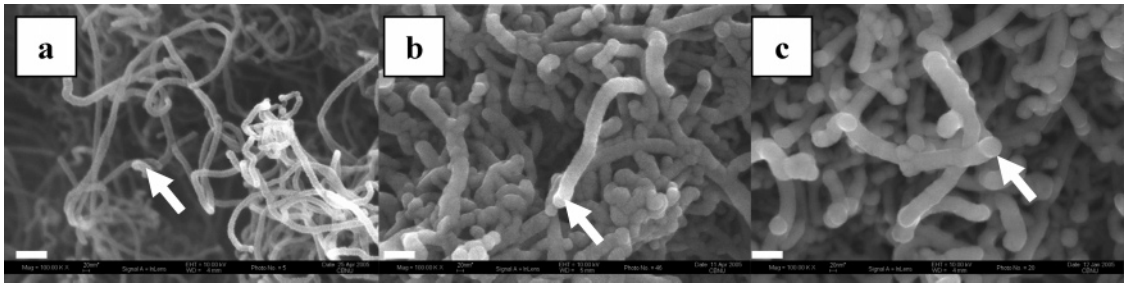

Figure 2. SEM images of (a) as-received MWNT from Iljin Nanotech Co. (100 000×); (b) MeO-MWNT (100 000×); (c) EtO-MWNT (100 000×). Scale bar is 100 nm.

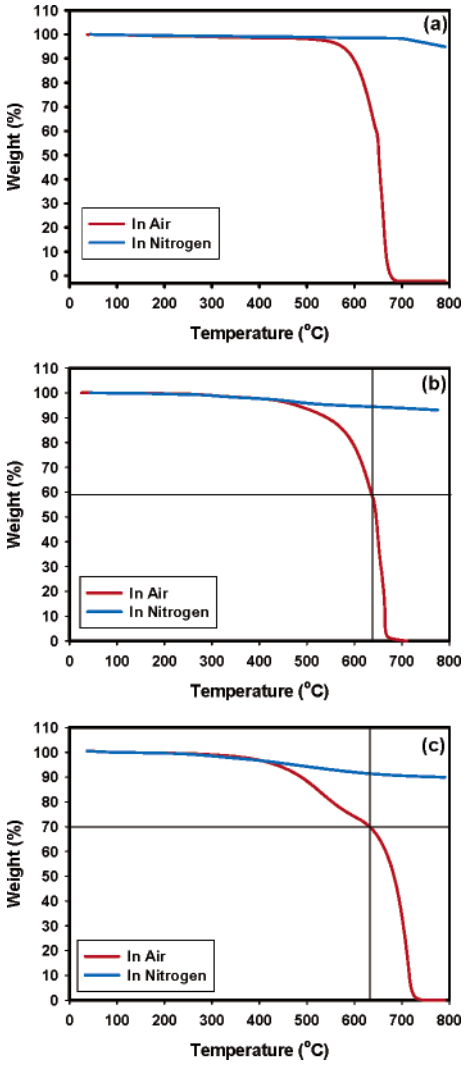

Figure 3. TGA thermograms obtained with heating rate of 10 °C/min: (a) MWNT, (b) MeO-MWNT, (c) EtO-MWNT.

the polymerization of ethylene glycol (EG) and terephthalic acid (TPA) in the presence of a functionalized (MeO-MWNT or EtO-MWNT) or unmodified MWNTs was carried out to generate *in situ* the respective MWNT/PET nanocomposite. Thus, the respective MWNTs (approximately 0.4 wt % based on the resultant nanocomposites) were first dispersed in EG with about 20 mol % excess with respect to the stoichiometric requirement of the comonomer (TPA). All polymerization experiments were conducted under EG reflux temperature. During the latter stage of the polymerization process at elevated temperature, excess EG was distilled off to achieve the stoichiometric (EG:TPA) balance. At the end of reaction,

Scheme 2. *In Situ* Polycondensation of EG Containing Approximately 0.4 wt % of Virgin MWNT, MeO-MWNT, and EtO-MWNT and TPA.

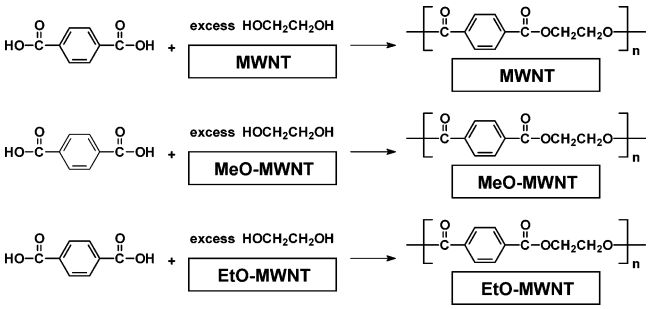

the resulting nanocomposites, while still in molten state at 295 °C, were extruded with a pressure of 1.5−3.0 kgf/cm^2 into cold water to form a continuous wire of approximately 2-mm diameter (Figure 4a). The wire was cut into chips 3−5 mm in length (Figure 4b−d). Uniform EtO-MWNT/PET nanocomposite films could also be cast from molten sample passing through the die of a calendaring extruder (Figure 5). The MWNT/PET (Figure 4b) nanocomposite was macroscopically heterogeneous. The aggregates of unmodified MWNT could be seen with naked eyes. Although MWNT could be physically dispersed in EG using homogenizer, its sedimentation occurred after a couple of hours of standing. While MeO-MWNT was dispersed more uniformly in EG than pristine MWNT, however, some sedimentation occurred in both pristine MWNT and MeO-MWNT samples after the dispersion in EG had been allowed to stand for a few hours. In sharp contrast, EtO-MWNT was well dispersed in EG and remained as a homogeneous mixture for a long time upon standing. Furthermore, the viscosity of the mixture was drastically increased, even with the addition of less than 0.2 wt % of EtO-MWNT, indicating that EtO-MWNT was fully swollen and/or dissolved, driven by certain strong interactions between EtO-MWNT and EG. The solution behavior could be originated from the structural similarity between ethoxy groups on EtO-MWNT and $-OCH_2CH_2O-$ fragments of EG molecules. Unlike MWNT/PET and MeO-MWNT/PET, the EtO-MWNT/PET nanocomposite was macroscopically homogeneous (Figure 4: a and d).

Thermal Properties. The DSC samples of all resultant nanocomposites were subjected to heating from room temperature to 285 °C with the same rate of 10 °C/min, quenched to 20 °C, and heated to 285 °C again (Figure 6). The T_g value was taken as the midpoint of the maximum baseline shift from each run. The PET, MWNT/PET, MeO-MWNT/PET, and EtO-MWNT/PET nanocomposite samples respec-

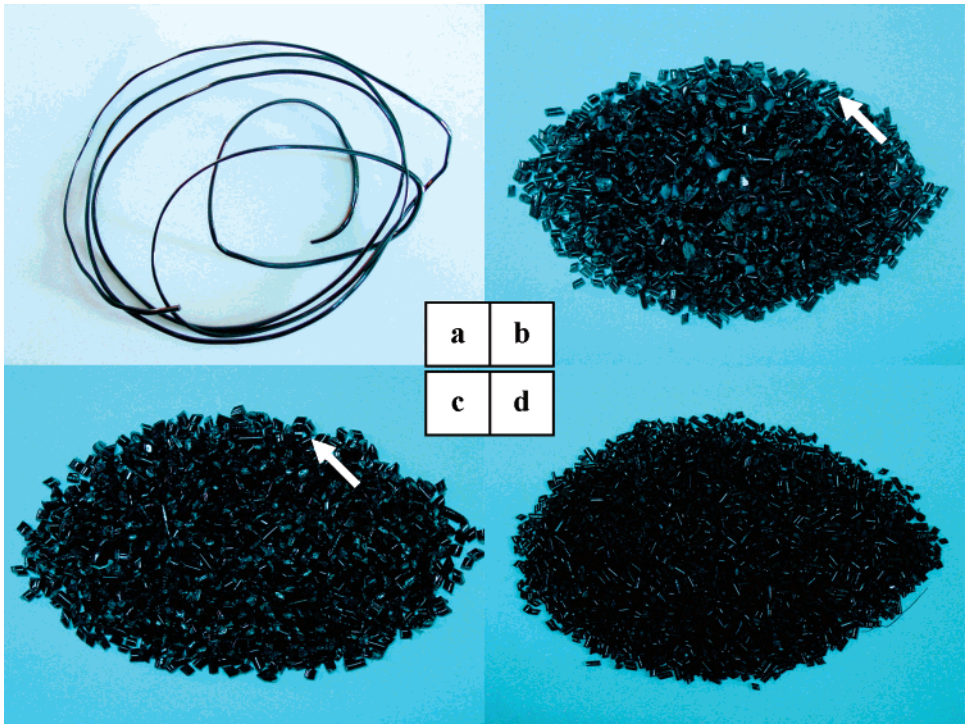

Figure 4. Digital photographs of (a) EtO-MWNT/PET wire, (b) MWNT/PET chips, (c) MeO-MWNT/PET chips, and (d) EtO-MWNT/PET chips. Arrowed chips are transparent with dark spots.

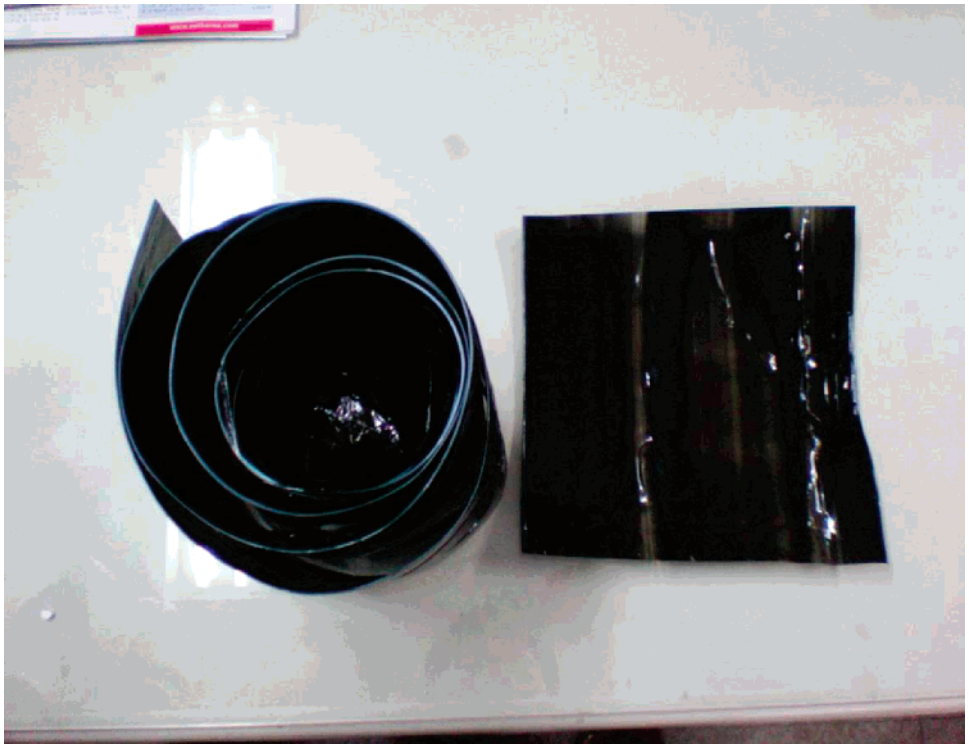

Figure 5. Digital photograph of EtO-MWNT/PET film cast from melt extrusion at 295 °C.

tively exhibited T_g's at 79.0, 73.8, 75.5, and 77.9 °C from the first heating run (Figure 6a) and 78.9, 78.5, 82.8, and 82.8 °C from the second heating run (Figure 6b). The T_g values of PET are almost identical from the first and the second heating scans. It is noteworthy that both MWNT and functionalized MWNT play as nucleating agents for PET to accelerate the rate of crystallization, while the samples were cooling after crystal melting. As a result of the increased crystallinity of these nanocomposites, the T_g's obtained for MWNT/PET, MeO-MWNT/PET, and EtO-MWNT/PET from their second runs were approximately 4.7, 7.3, and 4.9 °C higher than those from their first runs. Interestingly, the melting temperatures of MWNT/PET, MeO-MWNT/PET, and EtO-MWNT/PET nanocomposites, similar to the PET matrix, which showed T_m at 252.3 °C from the first heating scan and 250.9 °C from the second heating scan, were also respectively decreased from 253.8, 258.2, and 257.9 °C for the first run to 251.3, 255.5, and 255.4 °C for

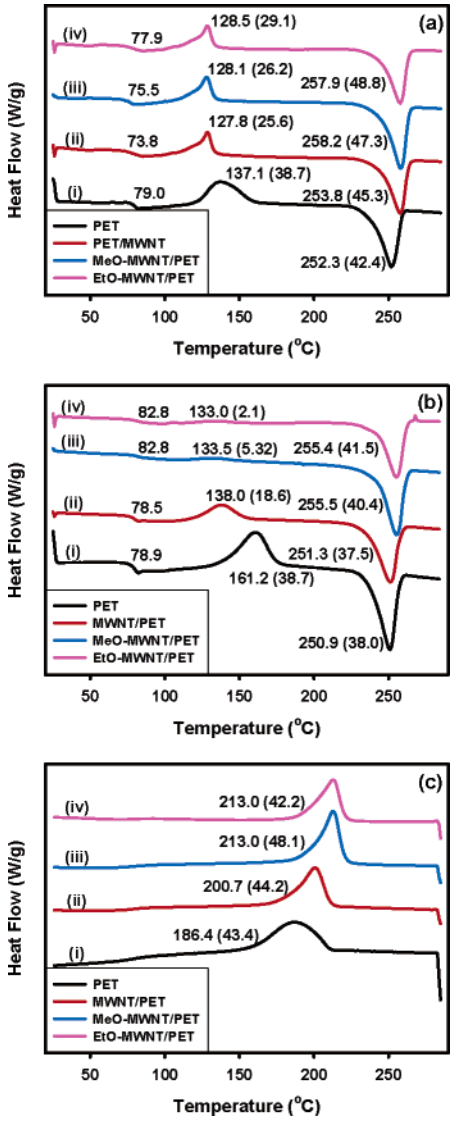

Figure 6. DSC thermograms obtained with heating and cooling rate of 10 °C/min: (a) the first heating scan, (b) the second heating scan, (c) the cooling scan after second heating. The numbers in parentheses are the amount of heat.

the second heating scan. Furthermore, both the cold (Figure 6b) and melt (Figure 6c) crystallization temperatures for MWNT/PET, MeO-MWNT/PET, and EtO-MWNT/PET nanocomposites provided supporting evidence that pristine MWNT and functionalized MWNT played as nucleating agents. Depicted in Figure 6c, MeO-MWNT/PET and EtO-MWNT/PET systems started to melt−crystallize at temperatures 26.6 °C higher than PET, indicating that crystal formation of both systems was thermodynamically more favorable than that of PET at higher temperature. The melt crystallization temperature of MWNT/PET system was also increased to 200.7 °C, but the increase (14.3 °C) was not as much as those of MeO-MWNT/PET and EtO-MWNT/PET systems. This might be due to the much poorer dispersion of pristine MWNT in PET matrix, resulting in less surface area of MWNT as the nucleation sites. This should be clearer from analyzing the cold crystallization temperature data (Figure 6b). MeO-MWNT/PET and EtO-MWNT/PET showed cold crystallization temperatures at 133.5 and 133.0 °C, respectively. There were only very small amounts (~2−5 J/g) of exothermic heat of crystallization for both systems detected by DSC, which meant a large portion of crystallization had already taken place while the samples were being quenched in a short time period. However, the MWNT/PET system still displayed 18.8 J/g of exotherm at 138.0 °C, indicating that MWNT had poor dispersion as well as poor interaction with the PET matrix. PET is a semicrystalline material with very slow crystallization rate after melting; the transparent PET films can be easily cast from its melt. Therefore, to impart maximal crystallinity to PET, it needs to be annealed above T_g for some finite amount of time. The relatively higher T_g, melting and crystallization temperatures from these nanocomposites can be interpreted by the roles that both functionalized and unfunctionalized MWNTs can serve as nucleating agents as well as fillers, accelerating crystallization rate to increase crystallinity.

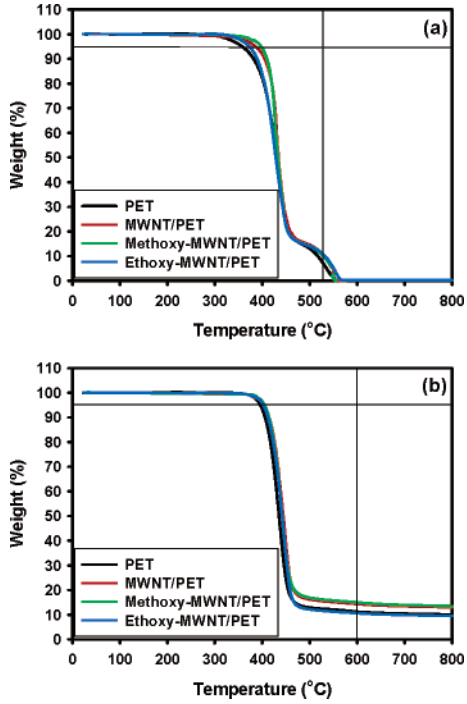

Figure 7. TGA thermograms obtained with heating rate of 10 °C/min: (a) in air and (b) in nitrogen.

Table 1. Thermogravimetric Analysis of PET, MWNT/PET, MeO-MWNT/PET, and EtO-MWNT/PET

	TGA			
	in air		in nitrogen	
composition (wt/wt)	$T_{d5\%}$	residue at 600 °C (%)	$T_{d5\%}$	residue at 530 °C (%)
PET (100)	358	6.6	396	11.2
MWNT/PET (0.4/99.6)	385	10.0	405	14.4
MeO-MWNT/PET (0.4/99.6)	398	9.8	405	15.0
EtO-MWNT/PET (0.4/99.6)	373	10.4	403	10.6

The TGA data obtained in both air and nitrogen are shown in Figure 7 and Table 1. The 5% weight loss of PET homopolymer was 358 °C in air and 396 °C in nitrogen. The retention weight percent of the residues at 530 °C in air are 6.6, 10.1, 8.8, and 10.4% for PET, MWNT/PET, MeO-MWNT/PET, EtO-MWNT/PET, in that order (Figure 7a). The residue percents at 530 °C in air for all the nanocomposite samples are more or less the same

(∼10 wt %) but much higher than the input amounts of pristine MWNT (∼1 wt %) and functionalized MWNT (0.59−0.70 wt %). The former fact seemingly confirms the lack of interfacial interaction between PET and the nanotubes in all the nanocomposites. Also, there is approximately 3 wt % more residues for the nanocomposite samples than the PET homopolymer. The amounts of residues in nitrogen at 600 °C are 11.2, 14.4, 15.0, and 10.6 wt % for PET, MWNT/PET, MeO-MWNT/PET, and EtO-MWNT/PET, respectively (Figure 7b). While we do not have a definitive explanation for these observations, we suspect that the significant increase in the amount of residues at 530 °C could be stemming from the carbonization of PET, forming amorphous carbon that appeared to be graphitized in nitrogen upon heating to 800 °C and beyond in the TGA experiments. Depending on the conditions, the pyrolysis of PET was reported to generate considerable amounts (16−67%) of carbonaceous residues.[13]

Scanning Electron Microscopy (SEM). The as-received MWNT surfaces are seamless and smooth (Figure 2a). The nanocomposite samples for SEM were fractured after their immersion in liquid nitrogen. In comparing the SEM images taken at the same magnification for MWNT/PET (Figure 8a), MeO-MWNT/PET (Figure 8b), and EtO-MWNT/PET (Figure 8c), it is clear that MWNT/PET system has poor MWNT dispersion, and MeO-MWNT/PET system has better dispersion. EtO-MWNT in PET matrix is homogeneously dispersed, and the interfacial boundary between EtO-MWNT and PET matrix is practically indiscernible. The aggregates in MWNT/PET nanocomposite can be seen with the naked eye (see Figure 4) and SEM images.

Since PET is stretchable while MWNT is not, EtO-MWNT/PET nanocomposite wire was strained approximately 300%, and the elongated neck area was fractured vertically and horizontally along the stretched direction. During the elongation process, the neck area was whitened as the result of an induced crystallization. Isolated EtO-MWNT coming out of PET matrix could be seen in the SEM image taken from horizontal fracture of the stretched sample (Figure 9a). However, the surface of isolated EtO-MWNT was heavily coated with PET (compare with Figure 2d), indicative of strong interfacial interactions between EtO-MWNT and the PET matrix. Moreover, it was hard to discern any isolated EtO-MWNT in the other area that was horizontally fractured. From the SEM image (Figure 9b) taken from vertical fractured surface, we were also unable to distinguish the boundary between EtO-MWNT and stretched PET. Thus, it could be concluded that EtO-MWNT/PET nanocomposite system is the best in terms of nanolevel dispersion among the three nanocomposite systems we obtained.

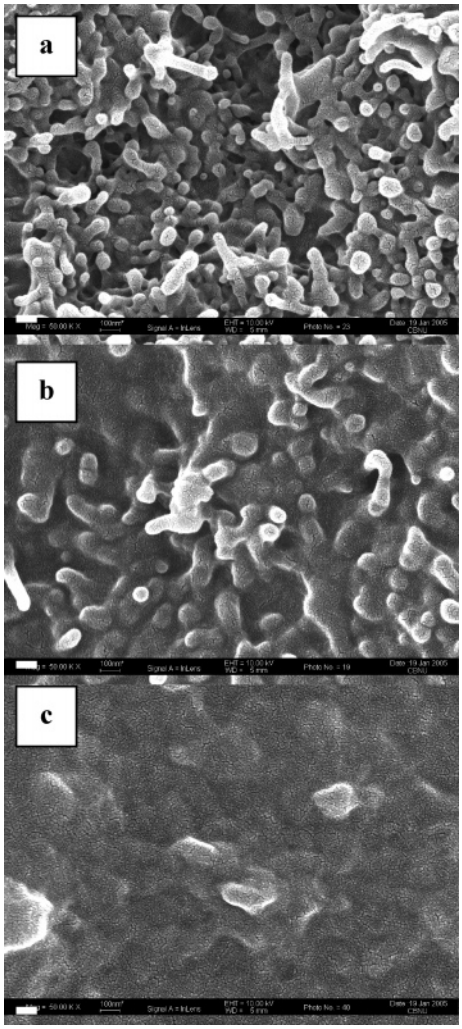

Figure 8. SEM images of (a) MWNT/PET (50 000×); (b) MeO-MWNT/PET (50 000×); (c) EtO-MWNT/PET (50 000×). Scale bar is 100 nm.

Concluding Remarks

Successful functionalization of multiwalled carbon nanotubes with alkoxybenzoyl pendants via Friedel−Crafts acylation in an optimized polyphosphoric acid has resulted in CNT materials with significantly enhanced compatibility with ethylene glycol. Most probably because of the structural similarity, ethoxybenzoyl-functionalized MWNT displayed prominently better dispersion in ethylene glycol than its methoxybenzoyl-functionalized counterpart. *In situ* polycondensations between the ethylene glycol and terephthalic acid in the presence of dispersed as-received MWNT, MeO-MWNT, or EtO-MWNT had resulted in high molecular weight poly(ethylene terephthalate) as the matrix for the resultant nanocomposites. As expected, EtO-MWNT/PET nanocomposite also exhibited the best dispersion and good interfacial interactions with the PET matrix. The resultant nanocomposites were easily fabricated into forms of wires, chips, films, and fibers via a simple melt extrusion at the final stage of an *in situ* polymerization process. The conductivity and radio frequency-resistance of their wires and films as a function of EtO-MWNT load are currently being investigated. Since our results have demonstrated the scale-up feasibility and processing convenience, the commercialization potential of MWNT/PET nanocomposites should be greatly enhanced.

(13) Masuda, T.; Miwa, Y.; Tamagawa, A.; Mukai, S. R.; Hashimoto, K.; Ikeda, Y. *Polym. Degrad. Stab.* **1997**, *58*, 315−320, and references therein.

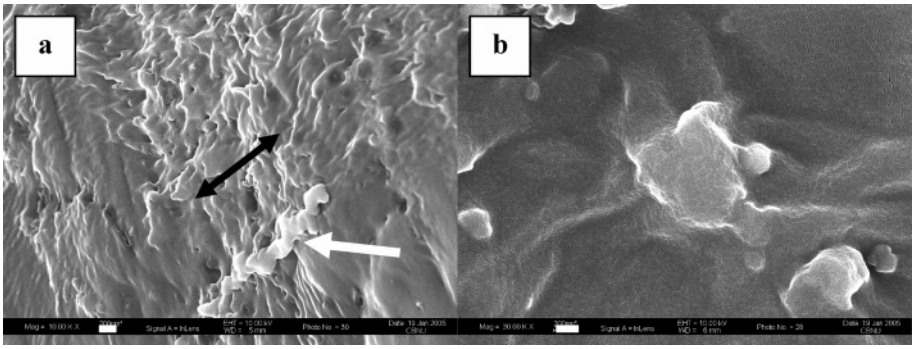

Figure 9. SEM images from (a) horizontal fractured surface of 300% strained EtO-MWNT/PET wire (10 000×, arrow is strain direction, scale bar is 400 nm); (b) vertical fractured surface of 300% strained EtO-MWNT/PET wire (30 000×, scale bar is 200 nm).

Experimental Section

Materials. All reagents and solvents were purchased from Aldrich Chemical Inc. and used as received, unless otherwise mentioned. MWNT (CVD MWNT 95) was obtained from Iljin Nanotech Co., LTD, Seoul, Korea.[14]

Instrumentation. Infrared (FT-IR) and Raman spectra were recorded on a Bruker Fourier-transform spectrophotometer (IFS-66/FRA106S). Elemental analysis was performed with a CE Instruments EA1110. Differential scanning calorimetry (DSC) was performed under the nitrogen atmosphere with heating and cooling rates of 10 °C/min using a TPA instrument model MDSC2910. The T_g values were taken from maximum inflections in baselines of the DSC traces. Thermogravimetric analysis (TGA) was conducted in nitrogen and air atmospheres with a heating rate of 10 °C/min using a TPA instrument SDT 2960 thermogravimetric analyzer. The field emission scanning electron microscopy (FESEM) used in this work was LEO 1530FE.

Representative Procedure for Functionalization. Into a 250 mL resin flask equipped with a high torque mechanical stirrer, nitrogen inlet and outlet, and 4-ethoxybenzoic acid (8.0 g, 48.1 mmol) were placed MWNT (8.0 g), P_2O_5 (50.0 g), and PPA (83% P_2O_5 assay; 200 g), and the mixture was stirred under dry nitrogen purge at 130 °C for 48 h. The initially dark mixture due to MWNT dispersion became lighter as the reaction progressed. At the end of the reaction, the color of the reaction mixture was shiny dark brown. The dope was poured into distilled water. The resulting powdery product was collected by suction filtration, washed with diluted ammonium hydroxide, Soxhlet-extracted with water for 3 days to remove residual PPA and with methanol for three more days to remove the unreacted 4-ethoxybenzoic acid, and finally vacuum-dried under reduced pressure (0.05 mmHg) at 100 °C for 48 h to give 12.3 g (81.0% yield) [Anal. Calcd for (EtO-MWNT) $C_{100}(C_9H_9O_2)_{3.5}$: C, 91.63; H, 1.56. Found: C, 91.18; H, 1.68.], to give 12.7 g (81.1% yield based on 100% conversion) [Anal. Calcd for (MeO-MWNT) $C_{100}(C_8H_7O_2)_{3.5}$: C, 91.81; H, 1.61. Found: C, 90.56; H, 1.48.], and to give 11.8 g (89.8% yield based on 100% conversion).

Representative Procedure for *In Situ* Synthesis of Poly(ethylene terephthalate) with 0.4 wt % MWNT Load). EtO-MWNT (0.4 g) was first dispersed in EG (40.0 g, 0.64 mol) and placed into a 250-mL resin flask equipped with a high torque mechanical stirrer, distillation apparatus with condenser, and nitrogen inlet and outlet. Then terephthalic acid (TPA, 83.0 g, 0.50 mol) was charged. The dark mixture was heated under reflux for 3 h at 250 °C for direct esterification, excess EG and water were distilled off, and then the mixture was heated to 280−295 °C for polycondensation. For comparison purpose, PET's containing virgin MWNT and 4-methoxybenzoyl-functionalized MWNT were also prepared with the same procedure used for EtO-MWNT/PET nanocomposite. In all the cases we obtained similar molecular weight ($[\eta] \sim 0.50-0.60$ dL/g in *o*-chlorophenol at 30 ± 0.1 °C). Final nanocomposite melts were extruded through a capillary die at 295 °C with 1.5−3.0 kgf/cm^2 pressure into cold water, forming a continuous wire, and the resulting wire was then cut into 2−3 mm chips with the aid of a cutting machine (see Figure 4). Anal. Calcd for $C_{10.06}H_8O_4$ (MWNT/PET): C, 61.36; H, 4.19. Found: C, 61.98; H, 4.24. Anal. Calcd for $C_{10.05}H_{7.05}O_{4.05}$ (MeO-MWNT/PET): C, 62.66; H, 3.70. Found: C, 61.69; H, 4.19. Anal. Calcd for $C_{10.05}H_{9.05}O_{4.05}$ (EtO-MWNT/PET): C, 62.01; H, 4.70. Found: C, 61.77; H, 4.19.

Acknowledgment. We are grateful to Jeong-Hee Lee (CBNU) for SEM, Woo-Jin Choi (CBNU) for TGA analysis, and Mee-Ja Sha (Saehan Industry Inc.) for DSC analysis. This project was supported by funding from US Air Force Office of Scientific Research, Asian Office of Aerospace R&D (AFOSR-AOARD) and Korea Research Foundation (R05-2004-000-10215-0).

CM051218T

(14) http://www.iljinnanotech.co.kr.